Experimental analysis of thermal runaway propagation behavior on 18650 lithium-ion battery under air and inert gas conditions

Pitsanusan Boonkit[1], Nontawee Petchsart[1], Supawut Apirakkitthworn[1] and Piyatida Trinuruk[1,*]

[1]*Department of Mechanical Engineering, King Mongkut's University of Technology Thonburi, Thailand*

*Corresponding author. Tel.: +66-2470-9114, Fax: +66-2470-9111

E-mail address: piyatida.tri@mail.kmutt.ac.th

Abstract

The applications of Lithium-ion batteries (LIBs) in a variety of industries have raised worries regarding the potential risks associated. Due to the battery may become violent when utilized in improper situations. Additionally, oxygen can enhance risk when a battery explosion occurs in the air, therefore it's crucial to mitigate the danger by displacing oxygen and preventing any reactions that may be dangerous. In this study, the thermal runaway (TR) process of the NMC LIBs 18650 was examined to find out how its behavior changed when interacting with helium instead of air. The fire behavior, temperature, pressure, gas produced, and energy raised were observed. The outcome demonstrated that the battery TR behaved similarly in both an air and helium environments. For the air environment, there were battery and gas explosions. The resulting product of the battery explosion powerfully reacted with the oxygen that existed in the air, triggering on a chain reaction and producing bright light. An environment temperature, pressure, gas generated, and energy raised of air tests were higher than helium. In contrast, the gas explosion in a helium environment was disappeared, leaving only a short jet fire occasion. The use of helium in this work improves battery safety during TR and can be advantageous from a propagation perspective as it lowers the likelihood of combustion by displaces oxygen and other reactive gases.

1. Introduction

Lithium-ion batteries (LIBs) have been widely used as energy storage in electronic products, electric vehicles [1], and grid storage [2] due to their excellent properties of high energy density, low self-discharge, and long-life cycle [3], [4]. However, LIBs components consist of reactive and flammable materials [5], which pose a risk and can be destructive. Therefore, battery safety concerns are spreading more widely. When batteries are operated improperly and abusively, including through thermal abuse, electrical abuse, and mechanical abuse, it may result in an explosion or fire that is related to thermal runaway (TR) from the battery.

Many research investigations on LIBs have been conducted in order to better understand the mechanism and characteristics of the LIBs hazards. The main cause of LIBs hazards has been discovered to be the TR, which occurred when an accumulation of heat generation rather than heat dissipation [6]. The heat generation is caused by the internal temperature and pressure increasing continuously, which triggers exothermic reactions inside batteries: the decomposition of solid electrolyte interface (SEI) layer, the reaction between the electrolyte and intercalated lithium at anode, Internal short circuit (ISC) caused by the separator collapse, and the exothermic reaction

decomposition of the cathode material and electrolyte [7]–[10].

There are many factors that influence the TR hazards. The thermal stability of cathode material directly influences the degree of safety. In general, the ranking of cathode material thermal stability becomes LiFePO$_4$ (LFP) > LiMnO$_4$ (LMO) > LiNi$_x$Co$_y$Mn$_z$O$_2$ (NCM) > LiCoO$_2$ (LCO) [11], [12]. The various SOC of LIBs has an immediate influence on the intensity of thermal runaway. The TR of fully charged LIBs presents the highest surface temperature [13]. The battery SOC increase, the TR hazard intensified, and more different types of exhaust gas constituents are released [14]. The primary contributing factor to TR is the instability of internal components, particularly the flammable organic electrolyte, which is the most commonly used in commercial LIBs such as ethylene carbonate (EC), dimethyl carbonate (DMC), propylene carbonate (PC), diethyl carbonate (DEC), ethyl methyl carbonate (EMC), and ethyl acetate (EA) [15]. However, the commercial LIBs using flammable organic liquid electrolytes cannot ensure their safety [16].

The risk associated with LIBs can be investigated from the perspective of fire propagation. When a battery undergoes TR, all of its flammable gases constitute the fuel, which primarily burns outside the battery and reacts with ambient oxygen. [17]. From this perspective, it is important to develop a novel to mitigate the fire propagation by reducing the oxygen concentrations. Zhao et al. [18] analyzed the TR behaviors under both enclosed and ventilated conditions. The gas explosion occurred with the limit of oxygen under enclosed condition. One of the commonly methodological which used to extinguish the fire and suppress explosion is inert gas dilution. Said et al. [19] investigated the TR propagation of 18650 LIBs arrays in both nitrogen and air environments to elucidate the impact of flaming combustion, The results showed that the TR propagation speed in air is higher than in nitrogen environments. Weng et al. [20] explored the effects of gas dilution of nitrogen and argon in efforts to mitigate TR and fire propagation. The study found that the TR propagation rate was reduced by 44% when the oxygen concentration was lowered from 21% to 12%. Li et al. [21] evaluated the effect of carbon dioxide dilution on flammability characteristics of the battery vent gas. They revealed that carbon dioxide can significantly reduce the battery vent gas flammability. However, Even the gas dilution was applied, batteries can go into TR and the temperature of batteries was still very high. This high temperature is indicating that the cooling performance of the mitigating agent is required [22].

Nevertheless, coupled conjugate research on the impact of inert gas dilution on battery fire and cooling performance is still limited. Ideal coolant properties such as high thermal capacity and high conductivity are preferred to enhance cooling performance. An extinguishing agent with low toxicity, non-conductive, and chemically inert are necessary to improve battery fire mitigation strategies. Thus, helium (He) is one of the inert gases that is appropriate in this circumstance. The chemical inertness, high specific heat, and thermal conductivity of helium make it an excellent coolant. Alipour et al. [23] proposed a novel helium-based battery thermal management system (BTMS) and compared cooling efficiency with air cooling. The findings demonstrated that helium gas is higher cooling effectiveness than air. Boonkit et al. [24] investigated the cooling performance of BTMS which used an inert gas instead of air as a coolant. They found that He had emerged as the most efficient coolant, resulting in the lowest average maximum temperature of any Reynolds number.

As stated above, plenty of studies have been done on the thermal behavior of batteries that conduct TR in an air environment. As well as a lot of research has focused on TR in a gas-dilution environment in order to determine how gas dilution lowers the risk from TR propagation. In this

research, an experiment was conducted on the TR of NMC LIBs 18650 in order to find out the different of TR behavior in air as compared to helium environments. Investigations focused into the effects of employing helium instead of air and its initial pressure. Helium was operated at pressures of 0, 1, 1.5, 2, 2.5, and 3 bars, and air worked at ambient pressure.
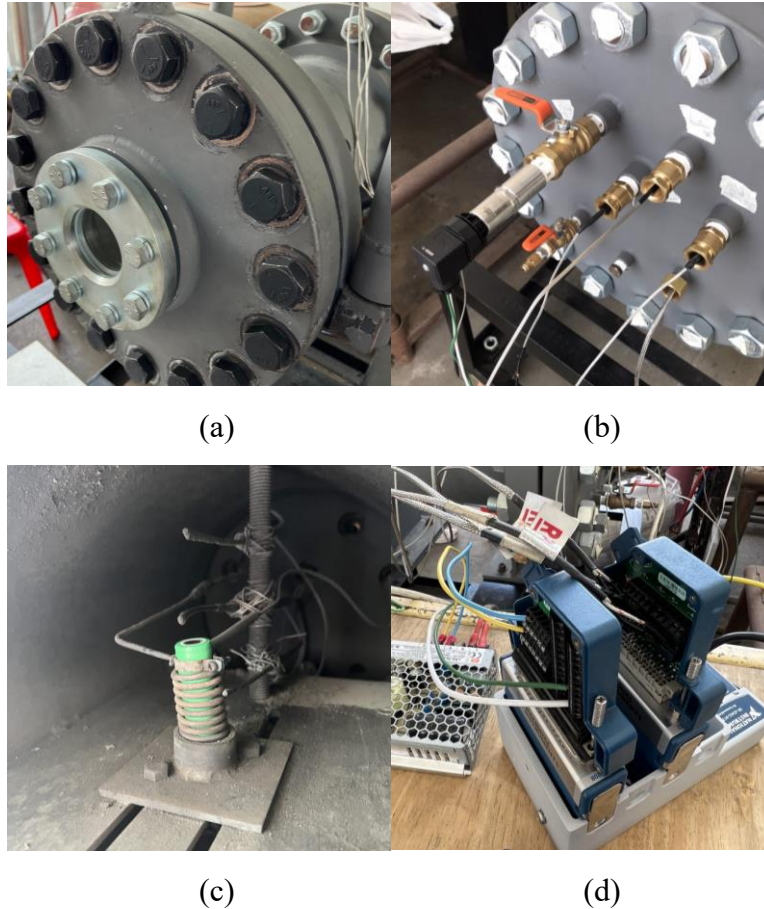
2. Experimental setup

2.1. Battery cell

Samsung INR18650-25R with Li-NiMnCoO2 (Lithium Nickel Manganese Cobalt Oxide) chemistry was employed in this experiment. The specification of battery cell is shown in **Table 1**. The battery cell was pre-cycled discharge at 0.5C-rate and finally fully charged (100% SOC) at 0.5C-rate.

Table 1 Specification of Samsung INR18650-25R

Parameters	Specification
Cathode	Li-Ni$_{1/3}$Mn$_{1/3}$Co$_{1/3}$O$_2$ (Lithium Nickel Manganese Cobalt Oxide)
Anode	Graphite
Nominal capacity (mAh)	2500
Nominal voltage (V)	3.6
Maximum cut-off voltage (V)	4.2
Minimum cut-off voltage (V)	2.5
Mass (g)	≤ 45

2.2. Experimental apparatus

<div align="center">(a)   (b)</div>

<div align="center">(c)   (d)</div>

Figure 1 Testing setup incliuding (a) the test chamber, (b) instrumentation port, (c) battery installation in support flame, and (d) data acquisition system.

The test chamber for TR experiment is shown in **Figure 1 (a)**. The body of the chamber is a seamless pipe made of ASTM A106 grade B, 10-NPT-size, schedule number 40, with a volume about 24 liters. The chamber interior has a diameter of 255 mm and a length of 470 mm. It can withstand a pressure of 25 bar. The cap of the chamber is blind flange class 300. The observation windows, with a diameter of 80 mm and a thickness of 20 mm, are set in the middle of the cap. The end cap is shown in **Figure 1 (b)**. It was drilled to use as an instrumentation port. One port is designed for a pressure transducer, which used to measure the pressure change in the chamber. One port is designed for heater wire. One port is designed for gas entry, which used to fill the helium gas in the chamber. The other four ports are designed for the introduction of k-type thermocouples. The illustration of the battery installation in support flame is shown in **Figure 1 (c)**. This section consists of a hot runner heater, with diameter and height are 20 mm and 50 mm, respectively. The support flame is 18 mm high, which can utilize for locking the heater. The two thermocouples T1 – T2 is used to measure the temperature of heater and battery, respectively. The other two thermocouples T3 – T4 is placed 10 mm and 50 mm away from the top of the battery. The data acquisition system is shown in **Figure 1 (d)**. It performed with a National Instruments (NI) cDAQ system and controlled by LabVIEW. The system record temperature and pressure data.
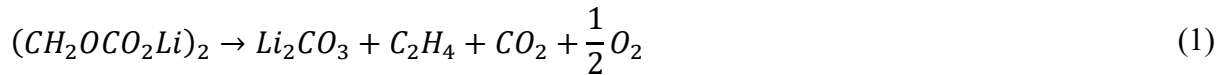
2.3. Experimental testing methods
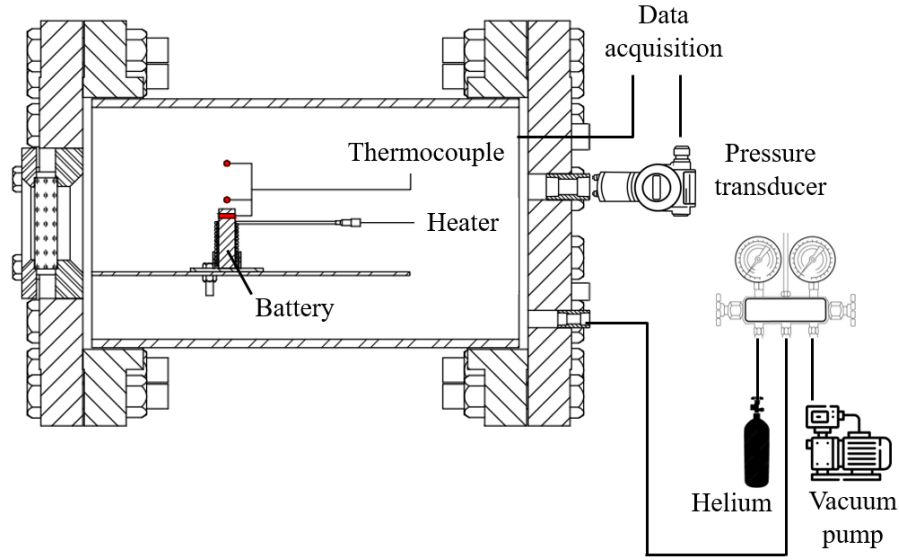
Figure 2 Schematic of test apparatus

Before the experiment, LIB was put on the support flame and placed with the hot runner heater. When the experiment conducting under air environment, the chamber was closed without vacuuming. Otherwise, in case of helium environment, the vacuum pump was used to reduce the pressure in chamber to zero. After that, the chamber was filled with helium at desired pressure operation. The camera position was adjusted to capture the TR and explosion process. In the experiment, heater was operated constant power at 110 W. After the battery goes to TR 5 second, heater was turned off.
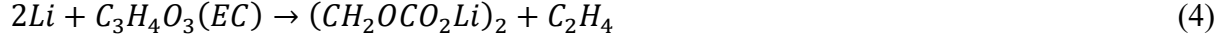
3. Methodology

3.1. Survey of typical reactions in LIBs

Many researches have reported the possible exothermic and chemical reactions that could occur inside the typical LIBs. They found that H_2, CO, CO_2, CH_4, C_2H_4 and C_2H_6 are the most common gases released from TR which offer a significant risk and toxicity [25]. As the temperature of the battery reaches about 69 °C [9], the decomposition of solid electrolyte interface (SEI) layer may occur firstly, and react with intercalated lithium to releases flammable gas. The possible reaction was described as following:
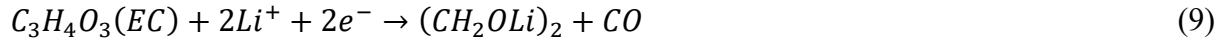
$$(CH_2OCO_2Li)_2 \rightarrow Li_2CO_3 + C_2H_4 + CO_2 + \frac{1}{2}O_2 \tag{1}$$

$$2Li + (CH_2OCO_2Li)_2 \rightarrow 2Li_2CO_3 + 2C_2H_4 \tag{2}$$

Without the protection of SEI, the electrolyte can react with the intercalated lithium. When the temperature of the battery reaches about 90 – 120 °C, the separator collapse, the cathode and anode contact together, followed by the internal short circuit (ISC). The electrolyte might react with intercalated lithium and produce hydrocarbon gas flammability [8], [9].
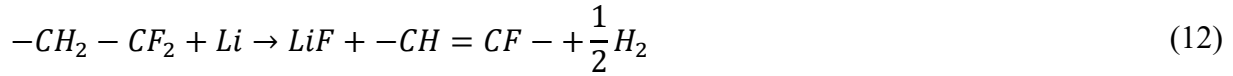
$$2Li + C_3H_4O_3(EC) \rightarrow Li_2CO_3 + C_2H_4 \tag{3}$$

$$2Li + C_3H_4O_3(EC) \rightarrow (CH_2OCO_2Li)_2 + C_2H_4 \tag{4}$$

$$2Li + C_3H_6O_3(DMC) \rightarrow Li_2CO_3 + C_2H_6 \tag{5}$$

$$C_3H_6O_3(DMC) + 2Li^+ + 2e^- + H_2 \rightarrow Li_2CO_3 + 2CH_4 \tag{6}$$
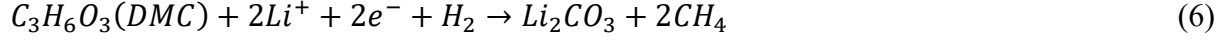
The oxygen released may react with electrolyte and produce CO_2

$$\frac{5}{2}O_2 + C_3H_4O_3(EC) \rightarrow 3CO_2 + 2H_2O \tag{7}$$

$$3O_2 + C_3H_6O_3(DMC) \rightarrow 3CO_2 + 3H_2O \tag{8}$$

The decomposition of electrolyte and reduction of CO_2 can also produce CO

$$C_3H_4O_3(EC) + 2Li^+ + 2e^- \rightarrow (CH_2OLi)_2 + CO \tag{9}$$

$$2C_3H_4O_3(EC) + 2O_2 \rightarrow 6CO + 4H_2O \tag{10}$$

$$2CO_2 + 2Li^+ + 2e^- \rightarrow Li_2CO_3 + CO \tag{11}$$

After 260 °C, the cathode material and Li will react with the binder and producing H₂

$$-CH_2 - CF_2 + Li \rightarrow LiF + -CH = CF - + \frac{1}{2}H_2 \tag{12}$$

$$CMC - OH + Li \rightarrow CMC - OLi + \frac{1}{2}H_2 \tag{13}$$

Another significant reaction is in the phase transition of the delithitated cathode material in LIBs. As temperature increases, the cathode material can decompose exothermically and release oxygen that can react exothermically with the electrolyte. This process is considered to be primarily responsible for the severity of the TR influence [26]–[28].

$$Li_xNi_{1/3}Co_{1/3}Mn_{1/3}O_2 \rightarrow Li_xNi_{1/3}Co_{1/3}Mn_{1/3}O_{2-y} + \frac{1}{2}yO_2 \tag{14}$$
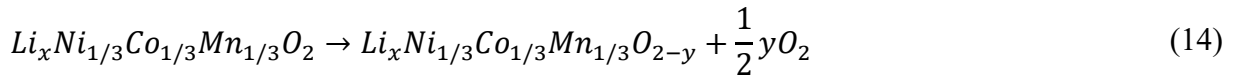
Following the battery TR phenomenon, the most common gases emitted is composed of 6 different gases (H₂, CO, CO₂, CH₄, C₂H₄ and C₂H₆). These gases have the ability to react with ambient oxygen, intensifying the hazards of post-TR. In this work, the reduced kinetics of hydrocarbon oxidation is considered by reaction mechanism [29].

$$H_2 + \frac{1}{2}O_2 \rightarrow H_2O \tag{15}$$

$$CH_4 + \frac{3}{2}O_2 \rightarrow CO + 2H_2O \tag{16}$$

$$C_2H_4 + 2O_2 \rightarrow 2CO + 2H_2O \tag{17}$$

$$C_2H_6 + \frac{5}{2}O_2 \rightarrow 2CO + 3H_2O \tag{18}$$

$$CO + \frac{1}{2}O_2 \rightarrow 2CO_2 \tag{19}$$
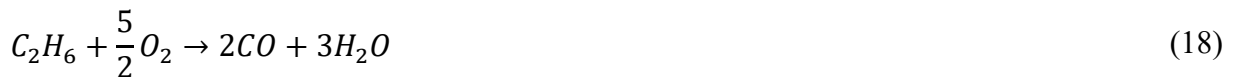
Due to the aforementioned reactions, it is important to investigate helium as a substance that might mitigate the risk of a battery TR. Because of non-reactive nature of helium property, reaction mechanism can be avoided. Helium reduces the possibility of combustion by displacing oxygen and other reactive gases and enhances battery safety during TR.

3.2. Model of energy conversion

When a battery was continuously heated, a gas was produced within the battery by a chain of exothermic and chemical processes. The establishment of temperature and pressure occurred until it reached a proper state, at the moment the onset of battery TR occurred. To investigate the battery TR in various environment, a fundamental energy conversion was used. The amount of gas generated from the battery was calculated by using the ideal gas law.

$$n = \frac{pV}{RT} - n_0 = \frac{pV}{RT} - \frac{p_0 V}{RT_0} \tag{20}$$

Where n is the amount of gas generated from the battery, n_0 is the initial amount of gas in the chamber at the beginning of the test (mol), p is the gas pressure (Pa), T is the gas temperature (K), p_0 is the initial gas pressure (Pa), T_0 is the initial gas temperature (K) (The gas temperature is average of two data, above the battery 10 mm and 50 mm), V is the volume of chamber, which is 0.0239 m³, and R is the ideal gas constant, which is 8.314 (J/mol/K).

During a battery TR occurs, an exothermic and chemical reactions release an enormous the amount of energy. This research evaluates the total energy released during battery TR phenomena by taking into factors including mass, specific heat capacity, and temperature. The total energy consists of two primary components: increasing the battery temperature and increasing the gas temperature [30]:

$$\Delta Q = \Delta Q_B + \Delta Q_G \tag{21}$$

Where ΔQ is the total energy (kJ), ΔQ_B is the energy raises the battery temperature (kJ), and the ΔQ_G is the energy raises the gas temperature (kJ).

$$\Delta Q_B = m_B c_{p,B}(T_{max} - T_0) \tag{22}$$

Where m_B is the mass of battery (kg), $c_{p,B}$ is specific heat capacity (kJ/kg/K), T_{max} is the maximum temperature of the battery (K) and T_0 is the initial TR temperature of the battery (K).

$$\Delta Q_G = m_G c_{p,G}(T_{max} - T_0) \tag{23}$$

Where m_G is the mass of gas in chamber (kg), $c_{p,G}$ is specific heat capacity of gas, which is 1.005 and 5.193 kJ/kg/K for air and helium, respectively, T_{max} is the maximum temperature of gas (K) and T_0 is the initial TR temperature of gas (K).
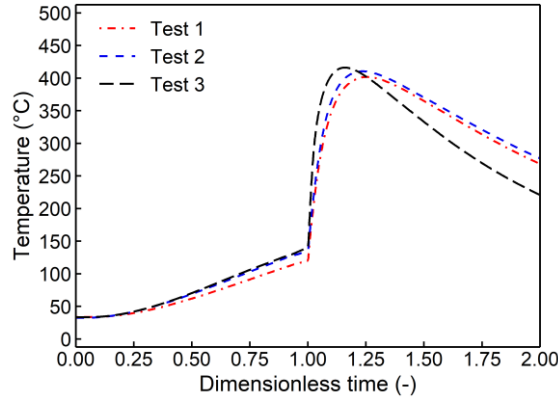
$$m_G = \rho V \tag{24}$$

$$p = \rho R_{gas} T \tag{25}$$

Where p is the initial pressure of gas (Pa), ρ is the density of gas (kg/m^3), and R_{gas} is the gas constant, which is 0.287 and 2.078 (J/kg/K) for air and helium, respectively.

## 4. Result and discussion

4.1. Repeatability of tests

Figure 3 The battery temperature profile in air experiments

The accuracy of experiment was investigated in order to ensure the repeatability of test. As shown in **Figure 3**, the battery temperature profile of the air experiments by three times indicated that the temperature behavior was very comparable. The time and temperature of the significant point from experiments; onset of safety venting and TR were observed in **Table 2**, which was calculated in term of mean, standard deviation, and %error. It was indicated that the average time for safety venting and TR of all cases were nearly the same with the error less than 12%, whereas the temperature for safety venting and TR of air case was fewer than all of helium cases with the error less than 8%. The error by time and temperature related to the accuracy of the thermocouple and AC electrical heater. From the summarized, the errors of experiment were acceptable.

Table 2 Summary of the experimental data about onset of safety venting and TR

| Case	t_{vent} (s)		T_{vent} (°C)		t_{onset} (s)		T_{onset} (°C)	
	Mean±SD	%Error	Mean±SD	%Error	Mean±SD	%Error	Mean±SD	%Error
Air 0 barg	187±17.06	9.12%	120.43±5.66	4.70%	206.92±23.93	11.56%	132.86±10.64	8.01%
Helium 0 barg	168±1.41	0.84%	129.46±1.07	0.83%	202±4.24	2.10%	144.13±6.36	4.41%
Helium 1.0 barg	184.08±15.27	8.30%	131.93±4.14	3.14%	218.75±17.93	8.20%	147.83±4.42	2.99%
Helium 1.5 barg	180±1.73	0.96%	131.51±2.73	2.08%	210.08±1.7	0.81%	143.85±3.56	2.47%
Helium 2.0 barg	183.42±11.63	6.34%	126.17±2.37	1.88%	218.83±16.06	7.34%	139.28±6.66	4.78%
Helium 2.5 barg	170±12.73	7.49%	134.59±0.25	0.19%	197.25±16.97	8.60%	146.96±3.04	2.07%
Helium 3.0 barg	185.33±17.21	9.29%	131.58±5.65	4.29%	216.25±21.47	9.93%	141.52±7.42	5.24%

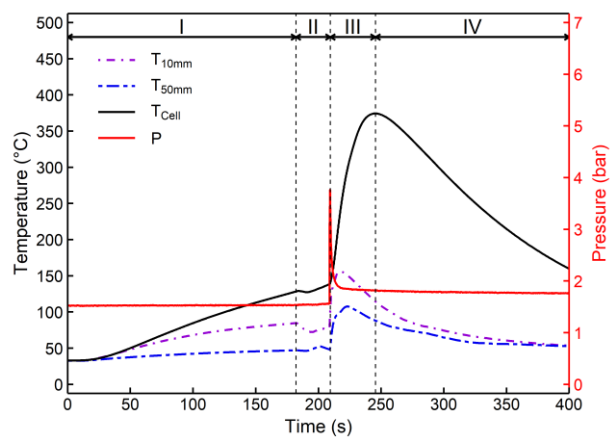*4.2. The thermal runaway characteristic of LIB*
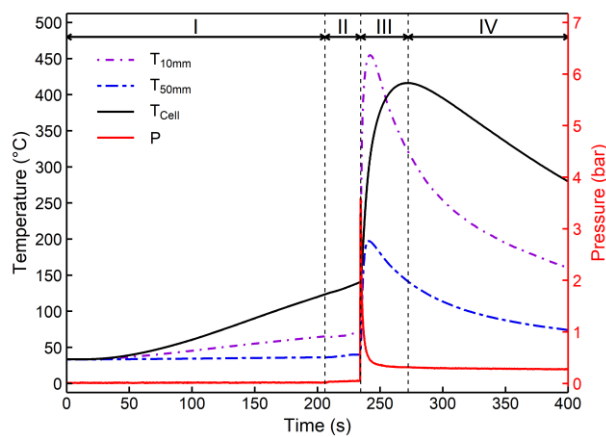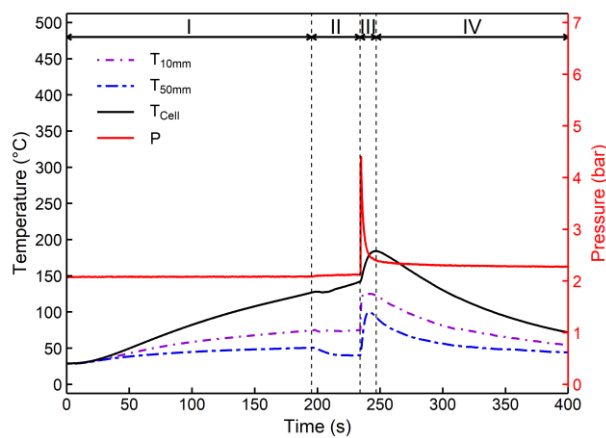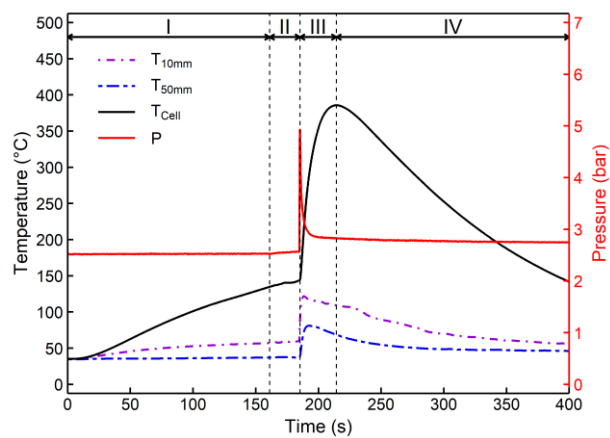
(a) Air 0 barg
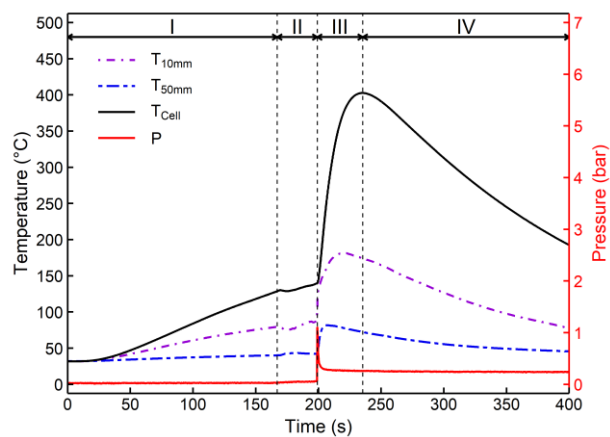
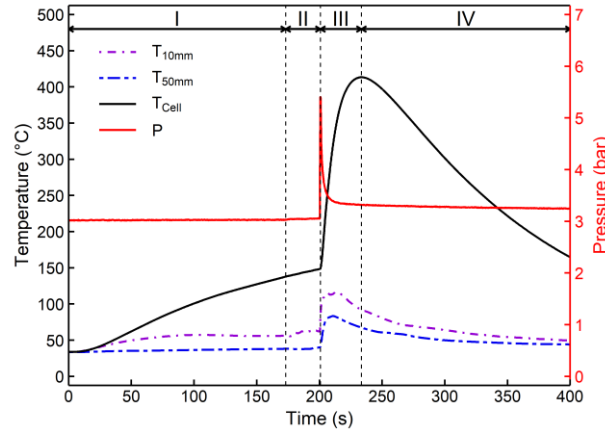(b) Helium 0 barg
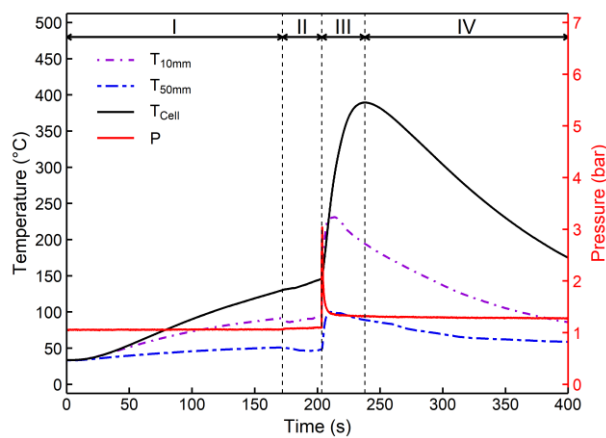
(c) Helium 1.0 barg

(d) Helium 1.5 barg

(e) Helium 2.0 barg

(f) Helium 2.5 barg

(g) Helium 3.0 barg

Figure 4 Thermal runaway characteristic under different conditions

Figure 4 presents the TR characteristic of LIBs at 100%SOC under different gas environments. Its divide into 4 stages; (I) heating, (II) venting, (III) thermal runaway, and (IV) decay.

Stage I (Heating): The battery cell was heated continually by the heater, causing its temperature to rise, which triggered a sequence of exothermic and chemical reactions, resulting in the accumulation of temperature and pressure within the battery.

Stage II (Venting): When the pressure inside a battery reaches a specific limit (Often 12-15 bars), a weak venting from the safety valve was observed, allowing hot flammable gases, electrolyte vapor, and aerosol droplets flow into the chamber quickly; as a result, the gas pressure was raised continually by approximately 1.2E-03 bar/sec, without noticeable difference in either case. At this point, the T_{Cell} dropped slightly due to Joule-Thomson expansion effect [31], especially in helium clearly show this behavior when compared with air, and then kept on increasing because of self-heating and heater effect. In this stage, previous research studies showed that the velocity of gas expelled at the safety valve can reach 457.1 m/s [32], causing the temperature above the battery cell T_{10mm} and T_{50mm} to fluctuated, particularly in helium when compared to air. After that, the temperatures continued to rise slowly.

Stage III (Thermal runaway): When the gas generated by the chemical reaction under suitable pressure and temperature, an explosion within the battery was occurred. A very short and weak venting was observed from the battery, followed by gas explosion in the chamber. The overall hazard from both of battery explosion and gas explosion reaction thus the gas pressure increased instantaneously as seen in **Table 3**. The average gas pressure raised in helium environment was less than air due to no combustion in the chamber. In air tests, the average gas pressure raised strongly by 4.32 barg, whereas in helium 0 barg tests, it rose the least, at 1.10 barg. Additionally, the gas pressure rise increased along with the increase in helium pressure.

In this stage, the T_{Cell} was continuously increased due to the burning of heat material within the battery until it reached its maximum temperature, which was between 370 – 420 °C in all cases. On the contrary, the behaviour of T_{10mm} and T_{50mm} are clearly different from T_{Cell}. Its increased rapidly especially in air test, which up to 472 °C, however, the maximum of T_{10mm} and T_{50mm} in

helium environments are lower than air, it was decreasing and became less and less as the helium pressure increased.

Table 3 The average maximum pressure and pressure differrent of all tests

Case	Maximum pressure (barg)	Pressure rise (barg)
Air 0 barg	4.33	4.32
Helium 0 barg	1.19	1.16
Helium 1.0 barg	3.11	2.03
Helium 1.5 barg	3.56	2.03
Helium 2.0 barg	4.26	2.22
Helium 2.5 barg	5.03	2.51
Helium 3.0 barg	5.77	2.73

Stage IV (Decay): The decay rate was a further important consideration. In air case, the battery has lower decay rates than helium case after reaching the peak temperature. This occurred because there was not a significant difference in temperature between the battery and its surroundings. In contrast, the helium scenarios showed an enormous temperature differential between the battery and its surroundings, when combined with helium's property such as high thermal conductivity relative to air, helium was capable of moving heat out of the cell faster than air.

In the heating stage, the T_{Cell} rise rate in air environments was slightly slower compared to helium, as shown in **Table 4**.

Table 4 The battery temperature rates in heating stage

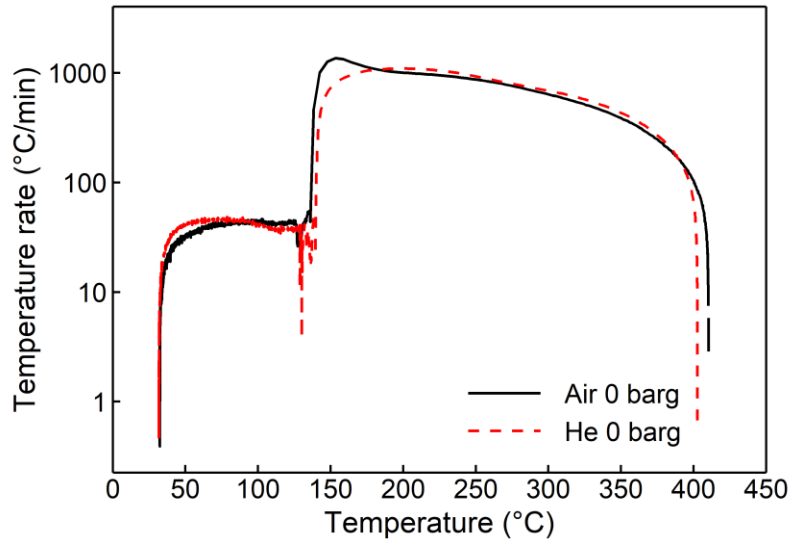| Case	Rate of T_{Cell} (°C/sec)
Air 0 barg	0.47
Helium 0 barg	0.58
Helium 1.0 barg	0.55
Helium 1.5 barg	0.54
Helium 2.5 barg	0.59
Helium 3.0 barg	0.54

In order to clarify the effect of gas environment in heating stage, the thermal diffusivity was calculated from experiment data as shown in **Table 5**.

$$\alpha = \frac{k}{\rho c_p} \qquad (26)$$

Where α is the thermal diffusivity (m²/s), k is the thermal conductivity (W/m/K), ρ is the density (kg/m³), and c_p is specific heat capacity (kJ/kg/K).

Table 5 Gas properties under conditions of absolute pressure of 1 bar at the beginning of the experiment

Fluid	Thermal conductivity (W/m/K)	Density (kg/m³)	Specific heat capacity (kJ/kg/K)	Thermal diffusivity (m²/s)
Air	0.027	1.166	1.005	0.023
Helium	0.157	0.164	5.193	0.185

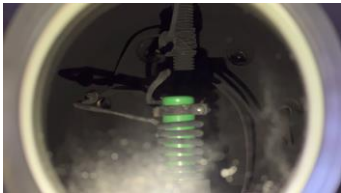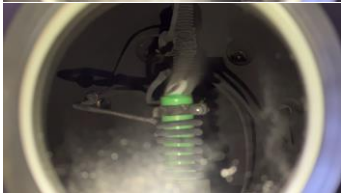**Figure 5** The rate of $T_{Battery}$ in air and helium environment with the pressure at 0 barg
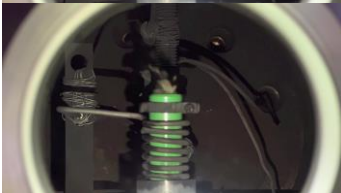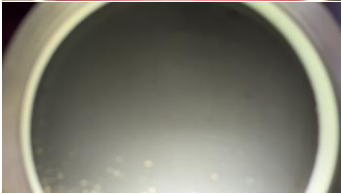
The rate of T_{Cell} TR in air and helium 0 barg environments were compared in **Figure 5**. It was shown that the rate of T_{Cell} in helium case higher than air. This was because the thermal diffusivity of helium was higher than air. The thermal energy from the heater can be transferred through helium faster than it was able to transfer across air. Therefore, when employing helium gas, the temperature nearly to the battery was higher than it would be with air. For instance, the T_{10mm} in helium case during the heating stage was higher than air, etc. The battery wasn't losing much heat in the helium case due to the fact that there wasn't much of a temperature difference between it and its surroundings. This results in a higher T_{Cell} and the rate of T_{Cell} in the helium case than the air case.

4.3. The gas explosion process in chamber

Figure 6 (a) depicts the complete battery explosion procedures in case of air, helium 0, and 2 barg. While **Figure 6 (b)** shows the sequence of gas explosion in chamber during the thermal runaway stage. It can be seen that the battery reacted strongly and emitted bright light in an air 0 barg environment. In contrast, the battery demonstrated a brief jet fire phenomena within a short time span in the helium environment. During the battery explosion, a reaction core formed as a result of the short and weak hot substances flow in the chamber, initiating the ignition of the
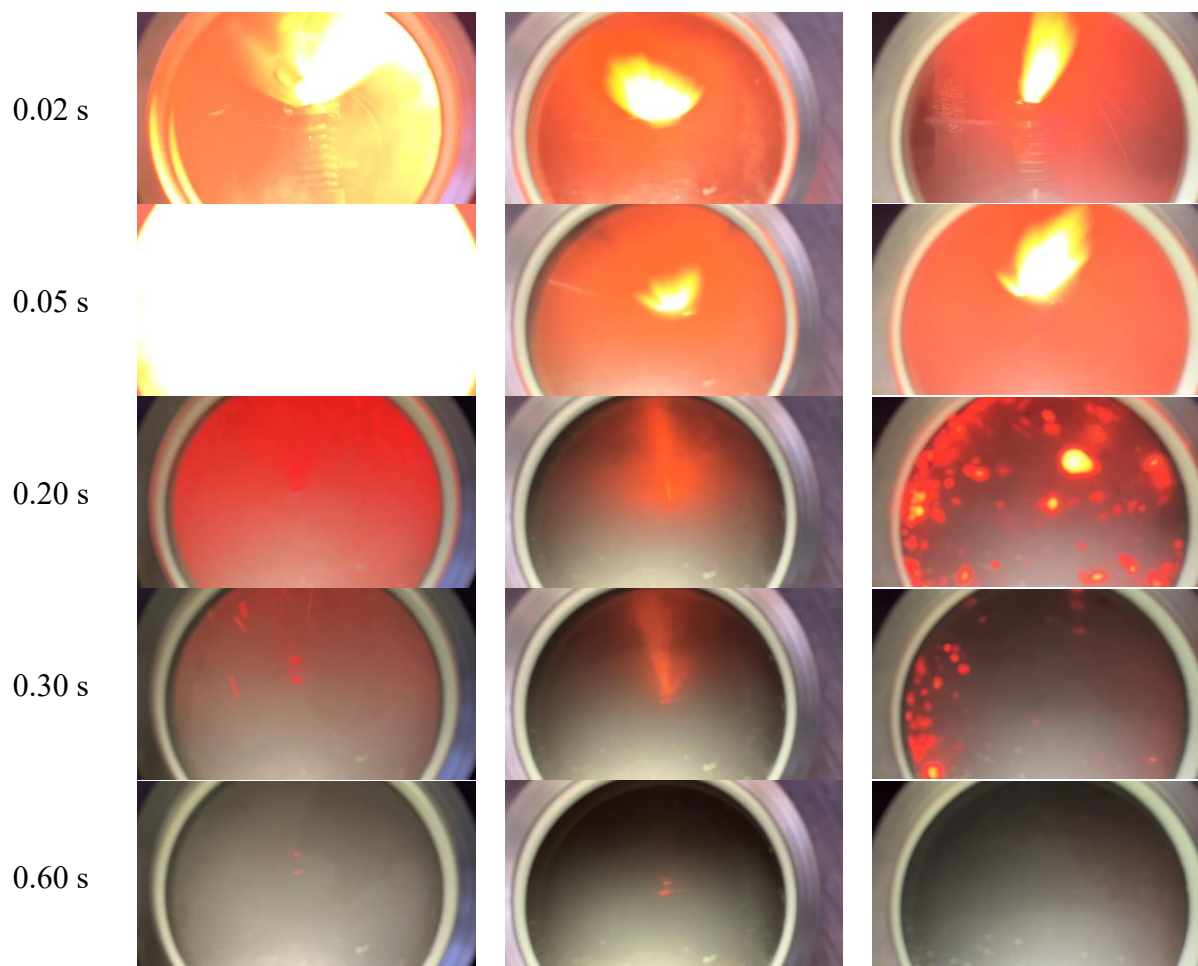
hydrocarbon gas flammability. This resulted in a chain reaction, in which the released energy started a self-sustaining sequential of reactions, resulting in a violent gas explosion and emission of intense light. In contrast, the experiments conducted in helium environments show a distinct behavior compared to air, with the lack of oxygen contributing to a reduction in the chain reaction, potentially leading to the suppression of the propagation of fire and associated hazards.

However, it's worth mentioning that the helium 2 barg environment presents a unique scenario. There's an ejection of heat material from the battery explosion is noticed, resulting in a significant temperature difference as compared to other situations. This phenomenon introduces an additional factor that can influence the battery explosion. The relation between reduced chain reaction propensity and heat material ejection will requires further exploration in order to fully comprehend the complex behavior observed under varied helium pressures.

(a) The complete battery explosion procedures
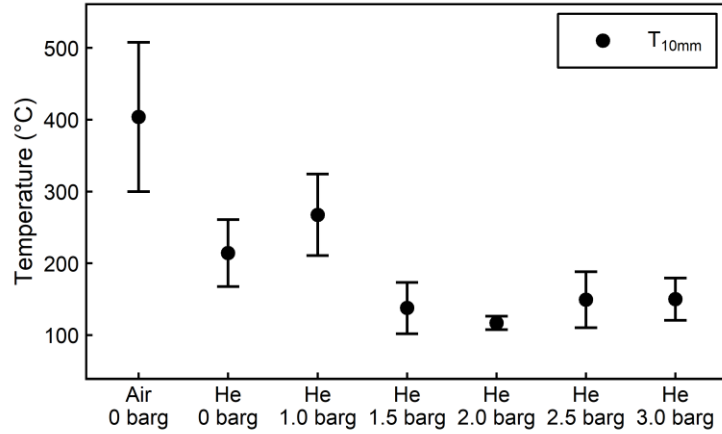
(b) The step of thermal runaway

Figure 6 The explosion process in chamber

4.4. The critical temperature analysis
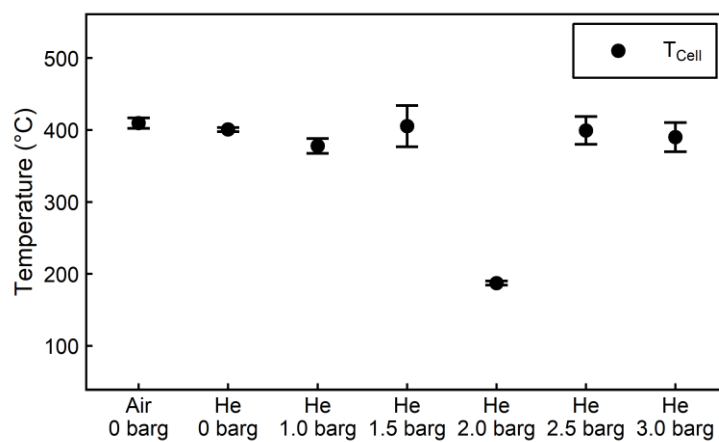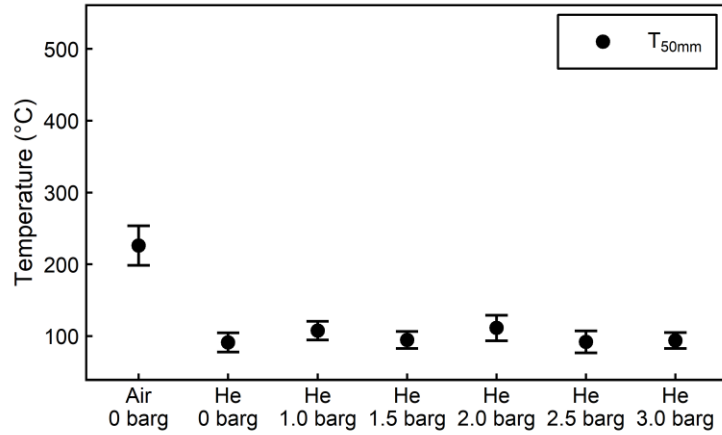

(a)

(b)

(c)

Figure 7 The average maximum temperature with error bar at (a) battery, (b) above 10 mm, and (c) above 50 mm.

Figure 7 shown the average maximum temperatures throughout all experiments conducted under each circumstance. It is clear that the average maximum T_{Cell} under all circumstances essentially remains the same, as illustrated in **Figure 7 (a)**. The average highest T_{Cell} in air scenario was 409 °C, which was a little higher than in helium environments cases, that ranged from 375 – 405 °C, with the exception of helium 2 barg, which was 187 °C due to heat material ejection from battery explosion.

The examination of the potential hazard from the battery explosion process by using temperature shows that changing the fluid environment had no influence on the hazard because one of the most important factors that affect the hazard of the battery explosion is state of charge (SOC), which was kept constant in this experiment. Previous research has shown that the phase transition of the cell cathode generate oxygen during the TR process, and the oxygen evolution is dependent on the cell SOC [33]. When the three fundamental components of combustion—oxygen, fuel, and heat—combine, batteries can also explode with a similar risk even if there is no oxygen in the surrounding environment when the fluid changes from air to helium.

Previous studies demonstrated that both the oxygen produced by the 100% SOC cell itself and some oxygen from the surrounding environment were totally consumed [34]. Then, battery explosion in helium environment had fewer hazards than air.

Figure 7 (b) and (c) shown the average maximum of T_{10mm} and T_{50mm} respectively. It is readily apparent that the T_{10mm} and T_{50mm} in the context of a battery explosion in air were higher than helium. The average maximum T_{10mm} in air environment was 404 °C, which was higher than helium, which ranged from 116 – 267 °C. Meanwhile, the T_{50mm} was 226 °C in the air case and ranged from 91 to 107 °C in helium. The findings from this study emphasizes the increased risk and related dangers when oxygen exists in the surrounding environment. This was caused by the previously mentioned about chain reaction. The chain reaction was significantly reduced when the fluid environment changed from air to helium, which prevented a violent gas explosion, only a short-lived jet fire phenomenon occurred for a short period of time.

4.5. Effect of helium by using energy conversion
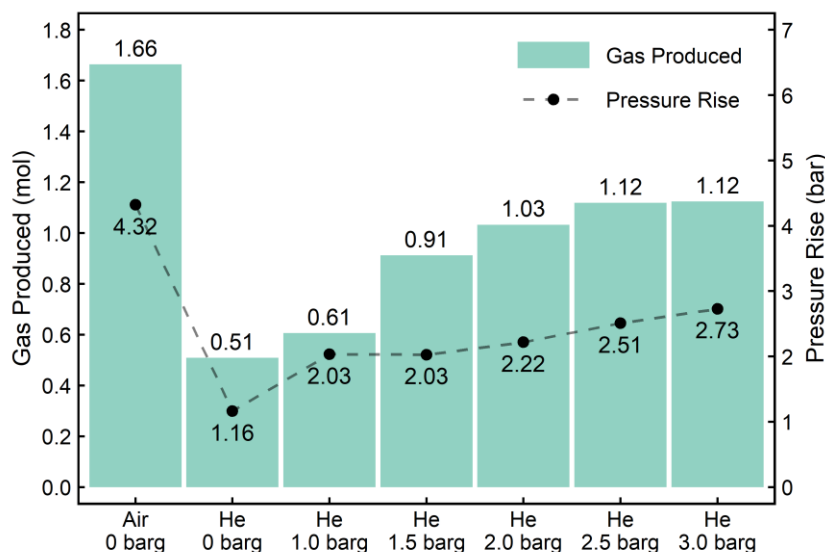
Figure 8 Correlation of the amount of gas generated from the battery

Figure 8 reveals the amount of gas generated from the battery. It can be noticed that the gas in air condition was largely produced at 1.66 mol. While in the helium 0 barg environment, the battery gas generated was modest at 0.51 mol and increases with increasing helium pressure, reaching 1.12 mol at helium 3 barg. The trend of the amount of gas generated was similar to the pressure rise. The average gas pressure rise considerably by 4.32 barg in air testing, but only 1.10 barg in helium 0 barg test.

The findings reveal that when helium pressure increases, consequently both the amount of gas generated and the pressure rise. It was possible to examine the helium pressure effect on a short and weak flammable gas venting at the beginning of the TR stage. When the helium pressure increased, it became more difficult to release a flammable gas, resulting in a more dangerous explosion within the battery. To summarize, increasing helium pressure does not lessen the

potential hazards of battery TR.
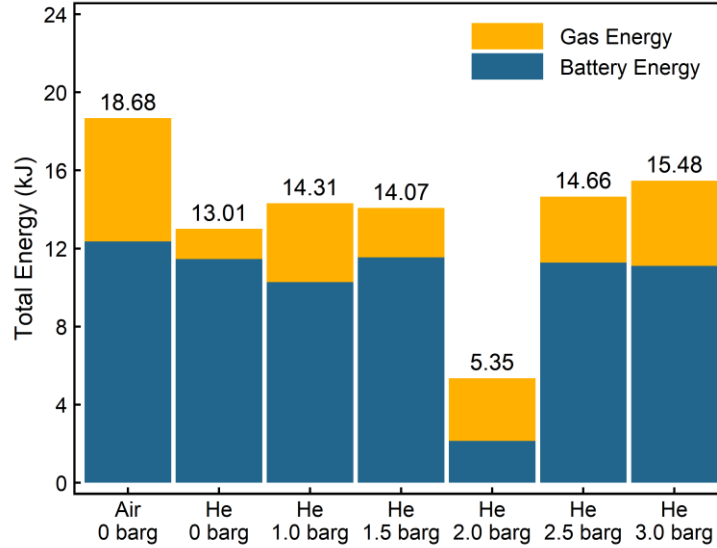
Figure 9 Correlation of the energy distribution

Figure 9 shows the evaluation of the average total energy released during battery TR of all tests in each condition. It can be noticed that a battery in an air environment releases the largest amount of total energy about 18.68 kJ, whereas batteries in helium situations release total energy between 13.01 – 15.48 kJ, with the exception of helium 2 barg, which was 5.35 kJ. Since the initial configuration of the battery were identical (SOC constant in all experiments), thus it thermal behaviour were same, its impact on energy-raised battery temperature was also consistent across all cases. However, the energy raising gas temperature had a distinct difference in comparison of air and helium environment. While the fluid in the chamber changed from air to helium, the gas energy rising decreasing from 6.32 kJ to a minimal of 1.55 kJ in helium 0 barg conditions.

Figure 8 and **Figure 9** demonstrate that there was an obvious distinction between fluid environments, air and helium. Because the oxygen in the air environment contributed to the chain reaction, which launched a series of self-sustaining reactions that led to the completed reaction mechanism (As shown in equation (15) - (19)), the battery explosion in air condition caused the most serious danger. This reaction resulted in the majority of gas generated and pressure rise, as same as the maximum gas energy during TR stage, which led to the propagation of fire and other hazard. While the battery explosion in helium environment shown that it can serves as a mitigation by displacing oxygen, which diminishes the gas generated, pressure rise, and gas energy during TR by decreasing of chain reaction. However, focusing on battery energy revealed that it was not always possible to mitigate the risk of a battery during a TR stage. Battery energy followed the same trend since a battery can be unsafe even if there is no oxygen in the surrounding environment but heating a battery can produce oxygen and initiate chemical reactions.

4.6. The error of setting experiment
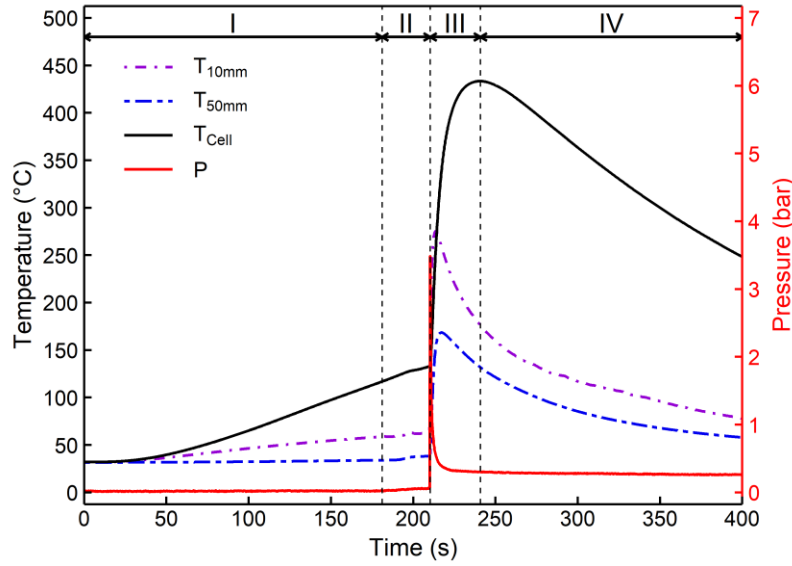
Figure 10 The error of setting before experiment

Relative humidity (RH) was an issue when conducting an experiment in a helium environment. As previously mentioned, a vacuum pump was utilized to lower the pressure inside the chamber to zero before helium gas was filled inside. In general, we vacuum approximately 20 to 30 minutes to guarantee that there was not any gas in the chamber. We conducted the experiment in the scenario of helium 0 barg with insufficient vacuuming (which is just 10 minutes) and a high RH environment outside the chamber. The result of battery TR was shown in **Figure 10**. It shown that the behavior of the TR was equivalent to the air case, particularly in terms of the pressure rise that is up to 3.49 bar. This was because of the gas explosion triggered by a reaction mechanism that required oxygen as a reactant. When the vacuuming duration was too short, oxygen from a high relative humidity was still present in the chamber, which led to a chain reaction and the fire propagation to the surrounding area.

5. Conclusion

In this research, an experiment was conducted on the TR of NMC LIBs 18650 in order to find out the different of TR behavior in air as compared to helium environments. The temperature and pressure for each air and helium environment at different initial pressures were crucial variables to figure out the severity of thermal runaway. The significant behaviors during TR stage were discussed, including the battery explosion, gas explosion, and total energy release. As a result of the experiment, the main conclusions can be summarized as follow:

- When the battery TR undergoes while its was surrounded by air or helium, the time for safety venting and the onset of TR is approximately the same in both environments, but the temperature is lower in the air cases.
- Battery TR phenomena occurred in both air and helium environments with similar stage. In the heating stage, the T_{Cell} rise rate in air environments was slightly slower compared to

helium as a result of thermal diffusivity. In the decay stage, helium was carried heat out of the cell faster than air.

- Because the battery can generate oxygen, the battery explosion proceeded similarly in both cases of air and helium. While the gas explosion in the air, the battery reacted strongly and generated bright light, resulting in a chain reaction. However, the gas explosion failed to appear in helium cases; instead, the battery exhibited a brief jet fire phenomenon in the helium environment, with the lack of oxygen leading to a decrease in the chain reaction.
- It was obvious that the average maximum T_{Cell} was almost constant under all conditions. However, in the context of a battery explosion in the air, the T_{10mm} and T_{50mm} were greater than helium.
- Only the air case of the battery experienced the gas explosion, which caused gas generated, pressure rise, and gas energy to be higher than in helium conditions.
- As the initial configuration of the battery were identical (SOC constant in all experiments), its thermal behavior remained similar across all scenarios, as was its effect on energy-raised battery temperature.
- When the vacuuming time was too short, oxygen from the high relative humidity remained in the chamber, causing a chain reaction and the fire to spread to the surrounding area.

Ref.

[1] M.-K. Tran *et al.*, "A Review of Range Extenders in Battery Electric Vehicles: Current Progress and Future Perspectives," *WEVJ*, vol. 12, no. 2, p. 54, Apr. 2021, doi: 10.3390/wevj12020054.

[2] B. Faessler, P. Kepplinger, and J. Petrasch, "Field testing of repurposed electric vehicle batteries for price-driven grid balancing," *Journal of Energy Storage*, vol. 21, pp. 40–47, Feb. 2019, doi: 10.1016/j.est.2018.10.010.

[3] T. C. Bach *et al.*, "Nonlinear aging of cylindrical lithium-ion cells linked to heterogeneous compression," *Journal of Energy Storage*, vol. 5, pp. 212–223, Feb. 2016, doi: 10.1016/j.est.2016.01.003.

[4] Q. Wang, B. Mao, S. I. Stoliarov, and J. Sun, "A review of lithium ion battery failure mechanisms and fire prevention strategies," *Progress in Energy and Combustion Science*, vol. 73, pp. 95–131, Jul. 2019, doi: 10.1016/j.pecs.2019.03.002.

[5] K. Liu, Y. Liu, D. Lin, A. Pei, and Y. Cui, "Materials for lithium-ion battery safety," *Sci. Adv.*, vol. 4, no. 6, p. eaas9820, Jun. 2018, doi: 10.1126/sciadv.aas9820.

[6] P. Liu *et al.*, "Thermal runaway and fire behaviors of lithium iron phosphate battery induced by over heating," *Journal of Energy Storage*, vol. 31, p. 101714, Oct. 2020, doi: 10.1016/j.est.2020.101714.

[7] B. Mao, H. Chen, Z. Cui, T. Wu, and Q. Wang, "Failure mechanism of the lithium ion battery during nail penetration," *International Journal of Heat and Mass Transfer*, vol. 122, pp. 1103–1115, Jul. 2018, doi: 10.1016/j.ijheatmasstransfer.2018.02.036.

[8] R. Spotnitz and J. Franklin, "Abuse behavior of high-power, lithium-ion cells," *Journal of Power Sources*, vol. 113, no. 1, pp. 81–100, Jan. 2003, doi: 10.1016/S0378-7753(02)00488-3.

[9] Q. Wang, J. Sun, X. Yao, and C. Chen, "Thermal Behavior of Lithiated Graphite with Electrolyte in Lithium-Ion Batteries," *J. Electrochem. Soc.*, vol. 153, no. 2, p. A329, 2006, doi: 10.1149/1.2139955.

[10] H. Yang, H. Bang, K. Amine, and J. Prakash, "Investigations of the Exothermic Reactions of Natural Graphite Anode for Li-Ion Batteries during Thermal Runaway," *J. Electrochem. Soc.*, vol. 152, no. 1, p. A73, 2005, doi: 10.1149/1.1836126.

[11] T. M. Bandhauer, S. Garimella, and T. F. Fuller, "A Critical Review of Thermal Issues in Lithium-Ion Batteries," *J. Electrochem. Soc.*, vol. 158, no. 3, p. R1, 2011, doi: 10.1149/1.3515880.

[12] J. Jiang and J. R. Dahn, "ARC studies of the thermal stability of three different cathode materials: LiCoO2; Li[Ni0.1Co0.8Mn0.1]O2; and LiFePO4, in LiPF6 and LiBoB EC/DEC electrolytes," *Electrochemistry Communications*, vol. 6, no. 1, pp. 39–43, Jan. 2004, doi: 10.1016/j.elecom.2003.10.011.

[13] Y. Fu, S. Lu, K. Li, C. Liu, X. Cheng, and H. Zhang, "An experimental study on burning behaviors of 18650 lithium ion batteries using a cone calorimeter," *Journal of Power Sources*, vol. 273, pp. 216–222, Jan. 2015, doi: 10.1016/j.jpowsour.2014.09.039.

[14] Q. Zhang, J. Niu, Z. Zhao, and Q. Wang, "Research on the effect of thermal runaway gas components and explosion limits of lithium-ion batteries under different charge states," *Journal of Energy Storage*, vol. 45, p. 103759, Jan. 2022, doi: 10.1016/j.est.2021.103759.

[15] G. G. Eshetu *et al.*, "In-depth safety-focused analysis of solvents used in electrolytes for large scale lithium ion batteries," *Phys. Chem. Chem. Phys.*, vol. 15, no. 23, p. 9145, 2013, doi: 10.1039/c3cp51315g.

[16] X. Tian *et al.*, "Design Strategies of Safe Electrolytes for Preventing Thermal Runaway in Lithium Ion Batteries," *Chem. Mater.*, vol. 32, no. 23, pp. 9821–9848, Dec. 2020, doi: 10.1021/acs.chemmater.0c02428.

[17] M. Chen, J. Liu, Y. He, R. Yuen, and J. Wang, "Study of the fire hazards of lithium-ion batteries at different pressures," *Applied Thermal Engineering*, vol. 125, pp. 1061–1074, Oct. 2017, doi: 10.1016/j.applthermaleng.2017.06.131.

[18] J. Zhao, S. Lu, Y. Fu, W. Ma, Y. Cheng, and H. Zhang, "Experimental study on thermal runaway behaviors of 18650 li-ion battery under enclosed and ventilated conditions," *Fire Safety Journal*, vol. 125, p. 103417, Oct. 2021, doi: 10.1016/j.firesaf.2021.103417.

[19] A. O. Said, C. Lee, S. I. Stoliarov, and A. W. Marshall, "Comprehensive analysis of dynamics and hazards associated with cascading failure in 18650 lithium ion cell arrays," *Applied Energy*, vol. 248, pp. 415–428, Aug. 2019, doi: 10.1016/j.apenergy.2019.04.141.

[20] J. Weng *et al.*, "Alleviation on battery thermal runaway propagation: Effects of oxygen level and dilution gas," *Journal of Power Sources*, vol. 509, p. 230340, Oct. 2021, doi: 10.1016/j.jpowsour.2021.230340.

[21] W. Li, H. Wang, Y. Zhang, and M. Ouyang, "Flammability characteristics of the battery vent gas: A case of NCA and LFP lithium-ion batteries during external heating abuse," *Journal of Energy Storage*, vol. 24, p. 100775, Aug. 2019, doi: 10.1016/j.est.2019.100775.

[22] S. Shahid and M. Agelin-Chaab, "A review of thermal runaway prevention and mitigation strategies for lithium-ion batteries," *Energy Conversion and Management: X*, vol. 16, p. 100310, Dec. 2022, doi: 10.1016/j.ecmx.2022.100310.

[23] M. Alipour, A. Hassanpouryouzband, and R. Kizilel, "Investigation of the Applicability of Helium-Based Cooling System for Li-Ion Batteries," *Electrochem*, vol. 2, no. 1, pp. 135–148, Mar. 2021, doi: 10.3390/electrochem2010011.

[24] P. Boonkit, N. Petchsart, S. Apirakkitthworn, and P. Trinuruk, "Improvement of cooling performance and mitigation of fire propagation in lithium-ion batteries using a novel gas-cooled thermal management system," *Inter J Ener Clean Env*, 2023, doi: 10.1615/InterJEnerCleanEnv.2023046956.

[25] A. W. Golubkov *et al.*, "Thermal-runaway experiments on consumer Li-ion batteries with metal-oxide and olivin-type cathodes," *RSC Adv.*, vol. 4, no. 7, pp. 3633–3642, 2014, doi: 10.1039/C3RA45748F.

[26] G.-H. Kim, A. Pesaran, and R. Spotnitz, "A three-dimensional thermal abuse model for lithium-ion cells," *Journal of Power Sources*, vol. 170, no. 2, pp. 476–489, Jul. 2007, doi: 10.1016/j.jpowsour.2007.04.018.

[27] R. Jung, M. Metzger, F. Maglia, C. Stinner, and H. A. Gasteiger, "Oxygen Release and Its Effect on the Cycling Stability of $LiNi_x Mn_y Co_z O_2$ (NMC) Cathode Materials for Li-Ion Batteries," *J. Electrochem. Soc.*, vol. 164, no. 7, pp. A1361–A1377, 2017, doi: 10.1149/2.0021707jes.

[28] A. W. Golubkov *et al.*, "Thermal runaway of commercial 18650 Li-ion batteries with LFP and NCA cathodes – impact of state of charge and overcharge," *RSC Adv.*, vol. 5, no. 70, pp. 57171–57186, 2015, doi: 10.1039/C5RA05897J.

[29] J. Kim, A. Mallarapu, D. P. Finegan, and S. Santhanagopalan, "Modeling cell venting and gas-phase reactions in 18650 lithium ion batteries during thermal runaway," *Journal of Power Sources*, vol. 489, p. 229496, Mar. 2021, doi: 10.1016/j.jpowsour.2021.229496.

[30] C. Zhao, J. Sun, and Q. Wang, "Thermal runaway hazards investigation on 18650 lithium-ion battery using extended volume accelerating rate calorimeter," *Journal of Energy Storage*,

vol. 28, p. 101232, Apr. 2020, doi: 10.1016/j.est.2020.101232.

[31] K. Zou, S. Lu, X. Chen, E. Gao, Y. Cao, and Y. Bi, "Thermal and gas characteristics of large-format LiNi0.8Co0.1Mn0.1O2 pouch power cell during thermal runaway," *Journal of Energy Storage*, vol. 39, p. 102609, Jul. 2021, doi: 10.1016/j.est.2021.102609.

[32] B. Mao, C. Zhao, H. Chen, Q. Wang, and J. Sun, "Experimental and modeling analysis of jet flow and fire dynamics of 18650-type lithium-ion battery," *Applied Energy*, vol. 281, p. 116054, Jan. 2021, doi: 10.1016/j.apenergy.2020.116054.

[33] B. Rowden and N. Garcia-Araez, "A review of gas evolution in lithium ion batteries," *Energy Reports*, vol. 6, pp. 10–18, May 2020, doi: 10.1016/j.egyr.2020.02.022.

[34] K. Zou, K. He, and S. Lu, "Venting composition and rate of large-format LiNi0.8Co0.1Mn0.1O2 pouch power battery during thermal runaway," *International Journal of Heat and Mass Transfer*, vol. 195, p. 123133, Oct. 2022, doi: 10.1016/j.ijheatmasstransfer.2022.123133.